J. Fluid Mech. (2003), *vol.* 477, *pp.* 259–283.

DOI: 10.1017/S0022112002003221 Printed in the United Kingdom

Internal wave resonances in strain flows

By STÉPHANE LEBLANC†

ANAM, Université de Toulon et du Var, BP 132, F-83957 La Garde cedex, France
and LEGI, Université Joseph Fourier, BP 53, F-38041 Grenoble cedex, France

(Received 31 January 2002 and in revised form 17 July 2002)

A simple mechanism of parametric excitation of internal gravity waves in a uniformly stably stratified flow under the inviscid Boussinesq approximation is presented. It consists in an oscillating planar irrotational strain field with frequency ω disturbed by three-dimensional plane waves. When the amplitude of the strain is weak, the problem is reduced to a Mathieu equation and a condition for parametric resonance is easily deduced. For a large-amplitude strain field equations are solved numerically with Floquet theory. In both cases, it is shown that parametric instabilities are excited when stratification is large enough, that is when $N > \frac{1}{2}\omega$, where N is the Brunt–Väisälä frequency of the flow. On the other hand, when $N \leqslant \frac{1}{2}\omega$, the flow is shown to be stable for any periodic background excitation thanks to a theorem by Joukowski. Therefore, stratification promotes instability. In the strongly stratified case $N \gg \omega$, resonant waves satisfy the Billant–Chomaz self-similarity law and the resulting instabilities develop inside correlated quasi-horizontal layers. After discussion of the viscous effects, the theory of the paper is applied to the stability of an elliptical vortex in a rotating stratified medium.

1. Introduction

In a uniformly rotating incompressible flow, inertial waves are known to propagate. Viewed from the rotating frame, wave motion is due to the restoring effect of the Coriolis force. When the background uniform rotation is slightly perturbed, such as by imposing a weak external strain field, it is now well known that those inertial waves are stretched periodically and their amplitude may grow exponentially, thanks to a mechanism of parametric resonance. The most celebrated example is the elliptical instability (Pierrehumbert 1986; Bayly 1986)‡, in which the parametric excitation of inertial waves is due to the ellipticity of the background flow, as explained by Waleffe (1990). Whereas the elliptical instability corresponds to an external steady strain superimposed to uniform vorticity, other kinds of background perturbation may lead to the parametric excitation of inertial waves: time-periodic external strains (Craik & Allen 1992; Bayly, Holm & Lifschitz 1996) or time-periodic compressions (Mansour & Lundgren 1990; Leblanc & Le Penven 1999) for instance. However, in each case the physical mechanism is the same and may be explained as follows: viewed in a relative frame which rotates with an angular velocity equal to half the vorticity of the

† Present address: LSEET, Université de Toulon et du Var, BP 132, F-83957 La Garde cedex, France.

‡ Discovered and rediscovered in various contexts-as reviewed recently by Kerswell (2002), the elliptical instability was identified in 1982 by Cambon in rapid distortion theory of homogeneous turbulence (see references in Cambon & Scott 1999).

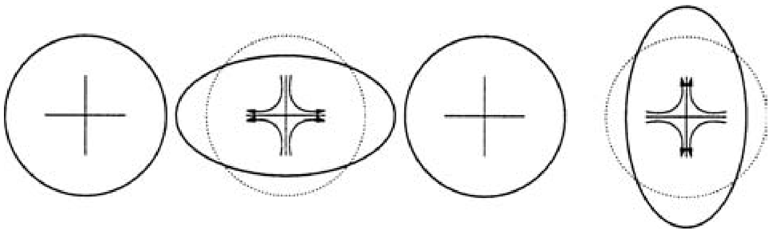

FIGURE 1. Schematic representation at different instants of the plane incompressible flow inside an elastic cylinder resulting from the periodic stretching of the boundary.

elliptic vortex, the background flow is irrotational but subject to an oscillating strain field, so that inertial waves may be excited parametrically.

Now, what happens in an incompressible flow at rest in a stably stratified medium? Because of the restoring effect of buoyancy, internal gravity waves propagate (LeBlond & Mysak 1978). Dynamics of internal gravity waves in stratified flows exhibit a variety of complex physical phenomena, such as the propagation of short gravity waves in a spatially varying flow, secondary instabilities and nonlinear triadic interactions of waves, mixing and small-scale turbulence (see the review by Staquet & Sommeria 2002). Keeping in mind the above discussion on the elliptical and related instabilities, our objective here is to isolate a simple basic mechanism of parametric excitation of internal gravity waves. The subject is not new and various theoretical and experimental studies have been carried out (McEwan & Robinson 1975; Sekerzh-Zen'kovitch 1983; Thorpe 1994; Benielli & Sommeria 1998). They are all based on the same principle: a closed container filled with a stably stratified flow is shaken in a periodic manner, so that viewed from the relative frame fixed to the container, the gravity field acting on the fluid particles is no longer constant, but time-periodic. As explained by Benielli & Sommeria (1998), the parametric excitation of the stable equilibrium of an oscillating pendulum may be interpreted in the same fashion.

The model proposed in the present paper is a little different: no external solid-body motion is imposed on the stratified flow, but the background flow itself experiences a time-periodic strain field in the horizontal plane, exactly as an irrotational two-dimensional flow inside a cylinder would be deformed periodically (see figure 1). As a consequence of the background strain, internal gravity waves are stretched, leading eventually to exponential growth of their amplitude when stratification is strong enough (the unstratified case is stable). Although this problem is rather academic, such a configuration might exist locally in more complex geophysical flows. Even if the mathematical treatment has some similarities, this model is even simpler than those presented by Miyazaki & Fukumoto (1992) or Majda & Shefter (1998) in that the stratified flows they consider are rotational, so that the instability mechanisms may be seen as a coupling between inertial and internal gravity waves. Parametric resonances also arise in the stability analysis of finite-amplitude internal waves as discovered by Mied (1976) and Drazin (1977); we do not know, however, whether these instability mechanisms have some link with the present work.

From a mathematical point of view, the problem may be reduced to a second-order ordinary differential equation with a time-periodic coefficient (a Hill equation), the theory of which relies on solid mathematical foundations (Cesari 1959; Yakubovich & Starzhinskii 1975). In particular, a theorem by Joukowski (Zhukovskii 1892)† will help

† His famous work on the lift of an airfoil was published a few years later in 1906.

us to determine with confidence a region of stability, outside of which internal waves are parametrically excited, leading to exponential growth of the amplitude. For weak strain, the problem reduces to a Mathieu equation for which good approximations of unstable solutions may be obtained with asymptotic methods (Bender & Orszag 1978). These results are compared to numerical computations, extending the study to large amplitudes of strain. As expected for such three-dimensional instabilities, viscosity is shown to be stabilizing.

Results of the paper are also discussed in the context of strongly stratified flows, for which some questions remain open. For instance, direct numerical simulations of forced stratified turbulence by Herring & Métais (1989) exhibit initial exponential growth of three-dimensional perturbations superimposed on a two-dimensionally forced turbulence, and the subsequent formation of horizontal layers. Billant & Chomaz (2000*a–c*) discovered a linear mechanism – the zigzag instability – which recovers some of the physics described above: exponential growth and layering. Furthermore, they pointed out the self-similarity of the perturbed flow for large stratification. Motivated by these observations, Billant & Chomaz (2001) proposed new scalings for strongly stratified inviscid flows, resulting in reduced dynamical equations of which the solutions are self-similar. It will be shown that our results confirm these features, and suggest an alternative mechanism for layer formation in strongly stratified flows.

The paper is concluded by a discussion on the stability analysis of an elliptical vortex in a rotating stratified medium, for which some results derived earlier may be directly applied. In particular, a condition for stability at zero absolute vorticity is deduced from Joukowski's theorem, thus extending the non-stratified case (Craik 1989; Cambon *et al.* 1994; Leblanc 1997). This complements previously published works on this topic (Gledzer & Ponomarev 1992; Miyazaki 1993; Kerswell 2002).

This work is arranged as follows: the equilibrium flow (§ 2); plane wave perturbations (§ 3); derivation of Hill's equation (§ 4); stability when $N \leqslant \frac{1}{2}\omega$ and Joukowski's theorem (§ 5); subharmonic resonance when $N > \frac{1}{2}\omega$ and asymptotic analysis (§ 6); higher-order resonances and numerical computations (§ 7); strong stratification and self-similarity (§ 8); the Billant–Chomaz scaling (§ 9); viscous damping (§ 10); discussion (§ 11); and epilogue: the elliptical instability in a rotating stratified flow (§ 12).

2. The equilibrium flow

Dynamics of a stably stratified flow in the inviscid Boussinesq approximation is described by (LeBlond & Mysak 1978):

$$(\partial_t + \boldsymbol{v}\cdot\nabla)\boldsymbol{v} + \nabla\varpi = q\boldsymbol{e}_z,$$
$$(\partial_t + \boldsymbol{v}\cdot\nabla)q + N^2\boldsymbol{v}\cdot\boldsymbol{e}_z = 0,$$
$$\nabla\cdot\boldsymbol{v} = 0,$$

where $\boldsymbol{v}$, ϖ, and q are, respectively, the velocity, kinematic pressure and buoyancy of the flow field. Stratification is assumed to be uniform along the vertical direction $\boldsymbol{e}_z$; the Brunt–Väisälä frequency N is therefore constant.

The flow defined by:

$$\boldsymbol{V}(\boldsymbol{x},t) = S(t)(x\boldsymbol{e}_x - y\boldsymbol{e}_y), \tag{2.1a}$$
$$\Pi(\boldsymbol{x},t) = \Pi_0(t) - \tfrac{1}{2}(S^2+\dot{S})x^2 - \tfrac{1}{2}(S^2-\dot{S})y^2, \tag{2.1b}$$
$$Q(\boldsymbol{x},t) = 0, \tag{2.1c}$$

is an equilibrium solution of the inviscid Boussinesq equations. It describes an unsteady irrotational strain field in the plane perpendicular to stratification (the overdot denotes time-derivative). The principal directions of strain are along the coordinate x- and y-axes. If we set:

$$S(t) = \dot{R}/R, \quad R(t) = 1 + \delta \sin \omega t, \tag{2.2}$$

with $0 \leqslant \delta < 1$ and $\omega > 0$ without lost of generality, (2.1) corresponds to an oscillating strain field with frequency ω and dimensionless amplitude δ. Particle flow trajectories in the (x, y)-plane are given by:

$$x(t) = x(0)R(t), \quad y(t) = y(0)/R(t),$$

so that if a fluid particle lies at the initial time on a circle of radius R_0 say, this circle is a material closed curve described at any time by:

$$x^2/R^2 + y^2R^2 = R_0^2,$$

which is the equation of an ellipse with time-periodically varying aspect ratio (see figure 1). Therefore, it is clear that the equilibrium flow (2.1) with (2.2) is also an exact solution inside an elastic cylinder (infinite along the z-direction) stretched in the (x, y)-plane, even in the viscous case.

When $\delta = 0$, the flow is at rest and internal gravity waves propagate. We shall now describe the dynamics of those waves under time-periodic solicitations. For this, equations of motions are linearized around the equilibrium state (2.1). By denoting:

$$\mathscr{S}(t) = \begin{pmatrix} S(t) & 0 & 0 \\ 0 & -S(t) & 0 \\ 0 & 0 & 0 \end{pmatrix}, \tag{2.3}$$

the velocity gradient of the equilibrium flow, any small perturbation is governed by:

$$(\partial_t + \boldsymbol{V} \cdot \nabla)\boldsymbol{v} + \mathscr{S}\boldsymbol{v} + \nabla\varpi = q\boldsymbol{e}_z, \tag{2.4a}$$

$$(\partial_t + \boldsymbol{V} \cdot \nabla)q + N^2\boldsymbol{v} \cdot \boldsymbol{e}_z = 0, \tag{2.4b}$$

$$\nabla \cdot \boldsymbol{v} = 0. \tag{2.4c}$$

It is also of interest to consider the evolution equation for the vorticity perturbation $\boldsymbol{\omega} = \nabla \times \boldsymbol{v}$ which reads:

$$(\partial_t + \boldsymbol{V} \cdot \nabla)\boldsymbol{\omega} = \mathscr{S}\boldsymbol{\omega} + \nabla q \times \boldsymbol{e}_z, \tag{2.5}$$

since the basic flow is irrotational. Therefore, we see immediately that:

(i) The vertical vorticity perturbation is conserved;

(ii) Two-dimensional perturbations are bounded;

(iii) The equilibrium flow is stable in the unstratified case.

Item (i) follows directly from (2.5). Item (ii) is a corollary of item (i), since for two-dimensional perturbations, vorticity is vertical and thus constant. Item (ii) is deduced from (2.2) and (2.3) for which (2.5) with $q = 0$ gives time-periodic solutions for the vorticity perturbation; this contrasts with the steady hyperbolic flow, unstable with or without stratification (Lagnado, Phan-Thien & Leal 1984; Friedlander & Vishik 1991). Note that items (ii) and (iii) imply boundedness of the vorticity perturbation; boundedness of velocity perturbation will be checked in the next section.

In the presence of viscosity, the vertical vorticity perturbation governed by a decoupled advection/diffusion equation is damped and decreases to zero; we will therefore neglect its effect in the paper. Further justifications will be given later.

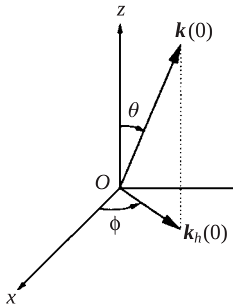

FIGURE 2. Initial orientation of the wave vector.

3. Plane wave perturbations

In the unbounded case, we shall look for plane wave solutions for the perturbation, sometimes called Lagrangian Fourier modes (Cambon & Scott 1999) or Kelvin waves (Kerswell 2002):

$$\boldsymbol{v}(\boldsymbol{x}, t) \equiv \boldsymbol{v}(t)\mathrm{e}^{\mathrm{i}\boldsymbol{k}(t)\cdot\boldsymbol{x}}, \tag{3.1}$$

and the same for pressure and buoyancy. The wave vector $\boldsymbol{k} = (\alpha, \beta, \xi)^T$ depends on time because it is stretched by the periodic background strain. System (2.4) must be valid for any $|\boldsymbol{x}|$, which is ensured when $\dot{\boldsymbol{k}} + \mathscr{S}\boldsymbol{k} = 0$, or equivalently:

$$\dot{\alpha}/\alpha = -\dot{R}/R, \quad \dot{\beta}/\beta = \dot{R}/R, \quad \dot{\xi} = 0,$$

leading to:

$$\boldsymbol{k}(t) = (k_0 \cos\phi \sin\theta/R(t),\ k_0 \sin\phi \sin\theta R(t),\ k_0 \cos\theta)^T, \tag{3.2}$$

where k_0 is an arbitrary positive constant, meaningless in the inviscid case since the unbounded problem exhibits no characteristic length scale; thus, we set $k_0 = 1$ throughout the paper, except when viscous effects will be taken into account. The (constant) angles θ and ϕ are the usual angles of spherical coordinates (figure 2); they characterize the orientation of the wave vector at the initial time. Note that $\boldsymbol{k}$ is time-periodic with period $2\pi/\omega$.

The amplitudes of velocity, pressure and buoyancy perturbations are governed by:

$$\dot{\boldsymbol{v}} + \mathscr{S}\boldsymbol{v} + \mathrm{i}\boldsymbol{k}\varpi = q\boldsymbol{e}_z, \tag{3.3a}$$

$$\dot{q} + N^2\boldsymbol{v}\cdot\boldsymbol{e}_z = 0, \tag{3.3b}$$

$$\boldsymbol{k}\cdot\boldsymbol{v} = 0, \tag{3.3c}$$

whereas the amplitude of the vorticity perturbation $\boldsymbol{\omega} = \boldsymbol{k}\times\boldsymbol{v}$ satisfies:

$$\dot{\boldsymbol{\omega}} = \mathscr{S}\boldsymbol{\omega} + q\boldsymbol{k}\times\boldsymbol{e}_z. \tag{3.4}$$

Since $\boldsymbol{k}\cdot\boldsymbol{\omega} = 0$, then $|\boldsymbol{\omega}| = |\boldsymbol{k}||\boldsymbol{v}|$. The wave vector being periodic, velocity and vorticity amplitudes have the same temporal behaviour, so that items (ii) and (iii) expressed in the previous section imply boundedness of both velocity and vorticity perturbations.

Before going into the heart of the problem, remember that each plane wave (3.1) is an exact nonlinear disturbance because of the orthogonality condition (3.3*c*). This well-known property (Bayly 1986; Craik 1989) is rather anecdotal since it is restricted to a single wave component propagating in an infinite domain.

4. Derivation of Hill's equation

We now show how to reduce the linear system (3.3) to a single second-order ordinary differential equation. For this, let

$$\mathscr{S}_h(t) = \begin{pmatrix} S(t) & 0 \\ 0 & -S(t) \end{pmatrix}$$

denote the horizontal part of the velocity gradient of the equilibrium flow. Splitting the velocity perturbation and the wave vector into horizontal and vertical parts:

$$\boldsymbol{v} = \boldsymbol{v}_h + w\boldsymbol{e}_z, \quad \boldsymbol{k} = \boldsymbol{k}_h + \xi\boldsymbol{e}_z,$$

and eliminating pressure from (3.3a), it is not difficult to show that the vertical velocity is governed by:

$$\frac{\mathrm{d}w}{\mathrm{d}t} = 2\xi\frac{\boldsymbol{k}_h \cdot \mathscr{S}_h\boldsymbol{v}_h}{|\boldsymbol{k}|^2} + \frac{|\boldsymbol{k}_h|^2}{|\boldsymbol{k}|^2}q. \tag{4.1}$$

Now, it may be shown that†:

$$\boldsymbol{k}_h \cdot \mathscr{S}_h\boldsymbol{v}_h = -\frac{\boldsymbol{k}_h \cdot \mathscr{S}_h\boldsymbol{k}_h}{|\boldsymbol{k}_h|^2}\xi w - \frac{\boldsymbol{k}_h \cdot \mathscr{S}'_h\boldsymbol{k}_h}{|\boldsymbol{k}_h|^2}\eta,$$

where $\eta = \boldsymbol{\omega} \cdot \boldsymbol{e}_z$ is the vertical vorticity perturbation which is constant ($\dot{\eta} = 0$) for an irrotational equilibrium flow, see (3.4), and

$$\mathscr{S}'_h(t) = \begin{pmatrix} 0 & S(t) \\ S(t) & 0 \end{pmatrix},$$

is the rotated strain tensor (Bayly *et al.* 1996).

Taking into account the expression of $\boldsymbol{k}_h$ in (3.2), we obtain $2\xi\eta\boldsymbol{k}_h \cdot \mathscr{S}'_h\boldsymbol{k}_h = KS$, where

$$K = 4\xi\eta\alpha(t)\beta(t). \tag{4.2}$$

Note that K is constant. Some manipulations also yields:

$$\frac{\mathrm{d}}{\mathrm{d}t}\log\frac{|\boldsymbol{k}_h|^2}{|\boldsymbol{k}|^2} = -2\xi^2\frac{\boldsymbol{k}_h \cdot \mathscr{S}_h\boldsymbol{k}_h}{|\boldsymbol{k}_h|^2|\boldsymbol{k}|^2},$$

so that equation (4.1) reads as:

$$\frac{\mathrm{d}w}{\mathrm{d}t} = \left(\frac{\mathrm{d}}{\mathrm{d}t}\log\frac{|\boldsymbol{k}_h|^2}{|\boldsymbol{k}|^2}\right)w + \frac{|\boldsymbol{k}_h|^2}{|\boldsymbol{k}|^2}q - \frac{KS}{|\boldsymbol{k}_h|^2|\boldsymbol{k}|^2}. \tag{4.3}$$

Together with the evolution equation for the buoyancy perturbation (3.3b), we obtain an inhomogeneous system of ordinary differential equations for w and q.

Keeping in mind the definition of K in (4.2), it is clear that the inhomogeneous term on the right-hand side of (4.3) vanishes for perturbations with zero vertical vorticity $\eta = 0$, which is physically realistic since in the presence of diffusion, the vertical vorticity vanishes at large times. Note that even if $\eta \neq 0$, K vanishes when the horizontal wave vector is aligned with one of the principal axes of strain ($\phi = 0$, π or $\pm\frac{1}{2}\pi$), leading to the most dangerous resonances as explained later. Therefore, we shall assume $\eta = 0$ without losing the main physical features of the problem.

† The case $|\boldsymbol{k}_h| = 0$, i.e. $\boldsymbol{k} = \boldsymbol{e}_z$, is stable, as may be easily deduced from (3.4).

System (3.3*b*) and (4.3) may now be reduced to a single homogeneous second-order equation for the rescaled vertical velocity perturbation p defined as:

$$p = \frac{|\boldsymbol{k}|^2}{|\boldsymbol{k}_h|^2} w.$$

Thus, we obtain the following system:

$$\frac{\mathrm{d}p}{\mathrm{d}t} = q, \quad \frac{\mathrm{d}q}{\mathrm{d}t} = -N^2 \frac{|\boldsymbol{k}_h|^2}{|\boldsymbol{k}|^2} p, \tag{4.4}$$

leading to

$$\frac{\mathrm{d}^2 p}{\mathrm{d}t^2} + N^2 \frac{|\boldsymbol{k}_h(t)|^2}{|\boldsymbol{k}(t)|^2} p = 0. \tag{4.5}$$

The ratio $|\boldsymbol{k}_h|^2/|\boldsymbol{k}|^2$ being periodic with period $2\pi/\omega$, (4.5) is a Hill equation. Note that this equation is valid for any symmetric uniform tensor $\mathscr{S}_h$, providing that $\eta = 0$.

When the background flow is at rest ($\delta = 0$), the wave vector is steady and (4.5) describes the propagation of plane internal gravity waves, with frequency $\pm N \sin\theta$ (LeBlond & Mysak 1978). Let us now characterize the unsteady case ($\delta \neq 0$). We first give a general criterion for stability.

5. Stability when $N \leqslant \frac{1}{2}\omega$; Joukowski's theorem

Floquet's theory asserts that (4.5) has normal solutions of the form (Cesari 1959):

$$p(t) = \mathrm{e}^{\gamma t} f(t),$$

where γ is the characteristic exponent that may be real or complex, and f is a periodic function with period $2\pi/\omega$. A bounded solution of (4.5) is said to be stable, and unstable otherwise. In the latter case, exponential growth occurs when $\mathrm{Re}(\gamma)$ is positive.

Beginning with Lyapunov, many results have been derived to test whether solutions of a Hill equation are stable or not; one of them (Borg's test) has been used by Bayly *et al.* (1996) to improve the stability of time-periodic elliptical flows. In our case, a particularly relevant stability test has been obtained by Joukowski (Zhukovskii 1892); we recall it below (Cesari 1959 p. 60; Yakubovich & Starzhinskii 1975 p. 697):

THEOREM (JOUKOWSKI). *The solutions of Hill's equation* $\ddot{p} + Q(t)p = 0$*, where* Q *is a real periodic function with period* T*, are all bounded provided*

$$j^2\pi^2/T^2 \leqslant Q(t) \leqslant (j+1)^2\pi^2/T^2, \tag{5.1}$$

for all t *and some integer* $j = 0, 1, 2, \cdots$.

The proof may be found in Yakubovich & Starzhinskii (1975). Note that this is a sufficient condition for stability. Applying Joukowski's theorem to our problem, we obtain:

COROLLARY 1. *Solutions of* (4.5) *with* (3.2) *are bounded if* $N \leqslant \frac{1}{2}\omega$.

The proof is immediate since $0 \leqslant N^2|\boldsymbol{k}_h|^2/|\boldsymbol{k}|^2 \leqslant N^2$ for any time, and $|\boldsymbol{k}_h|^2/|\boldsymbol{k}|^2$ has period $T = 2\pi/\omega$. If we assume $N^2 \leqslant \frac{1}{4}\omega^2$, then Joukowski's stability test (5.1) is satisfied for $j = 0$, so that the solution is bounded and the equilibrium flow is stable to perturbations with zero vertical vorticity, for any amplitude δ of the oscillating background strain. It is worth mentioning that this property holds also for any time-periodic function R in (2.2) with period $2\pi/\omega$.

Thus, a stability domain of Hill's equation, (4.5), has been determined with confidence, and we have found that the flow is stable when $N \leqslant \frac{1}{2}\omega$, i.e. for weak stratification. We will now explore the case of large stratification $N > \frac{1}{2}\omega$, and show that parametric instabilities develop. Before this, it appears useful in the following to introduce the rescaled time $t^* = \omega t$. Hill's equation thus reads:

$$\frac{\mathrm{d}^2 p}{\mathrm{d}t^{*2}} + n^2 \frac{|\boldsymbol{k}_h(t^*)|^2}{|\boldsymbol{k}(t^*)|^2} p = 0, \tag{5.2}$$

where

$$\frac{|\boldsymbol{k}_h(t^*)|^2}{|\boldsymbol{k}(t^*)|^2} = \frac{(\cos^2\phi + R^4(t^*)\sin^2\phi)\tan^2\theta}{R^2(t^*) + (\cos^2\phi + R^4(t^*)\sin^2\phi)\tan^2\theta}, \tag{5.3}$$

and $R(t^*) = 1 + \delta \sin t^*$. The frequency ratio

$$n = N/\omega,$$

is the important parameter of the problem. The flow is stable when $n \leqslant \frac{1}{2}$.

6. Subharmonic resonance when $N > \frac{1}{2}\omega$; asymptotic analysis

When the amplitude of the periodic background strain is weak, i.e. $\delta \ll 1$, after expanding (5.3) in powers of δ, equation (5.2) reduces to, at first order:

$$\frac{\mathrm{d}^2 p}{\mathrm{d}t^{*2}} + (a + 2\delta b \sin t^*)p = 0, \tag{6.1}$$

where

$$a(n,\theta) = n^2 \sin^2\theta, \quad b(n,\theta,\phi) = -n^2 \sin^2\theta \cos^2\theta \cos 2\phi, \tag{6.2}$$

which is, up to an irrelevant shift in time, a Mathieu equation. When $a > 0$ and $0 < \delta \ll 1$, solutions of (6.1) are bounded, except in the vicinity of resonances defined by (Bender & Orszag 1978):

$$a = \tfrac{1}{4} j^2 \quad (j = 1, 2, 3, \cdots),$$

where the solutions are exponentially growing with growth rate of order δ^j.

The first-order (subharmonic) resonance corresponds to $j = 1$, for which condition $a(n,\theta) = \frac{1}{4}$ leads to, from (6.2):

$$n > \tfrac{1}{2}, \tag{6.3}$$

since $\sin^2\theta < 1$ (the case $\sin^2\theta = 1$ corresponds to two-dimensional stable perturbations). Higher-order resonances arise when $n > \frac{1}{2}j$ with $j = 2, 3, \cdots$, for which condition (6.3) is always ensured. Their growth rate being much weaker than the subharmonic one, we shall restrict our study to the latter.

Multiple scale asymptotics provides an accurate description of subharmonic resonance for the Mathieu equation (6.1) when δ is small enough. For completeness of the presentation, we now review the main lines of this technique (for further details, see Bender & Orszag 1978). The necessity for it comes from the fact that if we look for a standard perturbative solution $p(t^*) = p_0(t^*) + \delta p_1(t^*) + \cdots$ of the Mathieu equation, and identify terms of the same order in δ, we obtain oscillating solutions for p_0 and p_1, except when $a = \frac{1}{4}$ which leads to secular (algebraic) growth for p_1. In the latter case, it is clear that the asymptotic expansion becomes disordered for time scales of order δ^{-1}. Therefore, to study the vicinity of $a = \frac{1}{4}$, we set $a = \frac{1}{4} + \delta a_1 + \cdots$, and look now for a solution such as:

$$p(t^*) = P_0(t^*, T^*) + \delta P_1(t^*, T^*) + \cdots,$$

where $T^* = \delta t^*$ is a slow time scale, considered in the analysis as an independent variable. At leading order, the Mathieu equation leads to:

$$P_0(t^*, T^*) = A(T^*)\mathrm{e}^{\mathrm{i}t^*/2} + \text{complex conjugate.}$$

The slowly evolving amplitude A is determined by demanding that secular terms be eliminated from the order δ solution (Bender & Orszag 1978). This leads to the following linearly independent solutions:

$$A(T^*) = A_\pm \exp\big(\pm T^* \sqrt{b^2 - a_1^2}\big),$$

showing that the solution of the Mathieu equation (6.1) grows exponentially when $|a_1| < |b|$, that is when:

$$\tfrac{1}{4} - \delta|b| < a < \tfrac{1}{4} + \delta|b|. \tag{6.4}$$

The maximum growth rate (in t^* units) is precisely $\sigma = \delta|b|$, reached at the middle of the interval defined by (6.4), i.e. for $a = \frac{1}{4}$ (or $a_1 = 0$). We recall that this first-order parametric resonance is called subharmonic since on the boundaries of the tongue of instability (put $|a_1| = |b|$ in the above discussion), the solution is periodic with period 4π (in t^* units), twice the period of the forcing term in the Mathieu equation (Cesari 1959).

Back to the physical problem, the above considerations together with (6.2) tell us that the most dangerous resonance is reached for the initial wave vector orientation $\theta = \bar{\theta}$ defined such that $n^2 \sin^2\bar{\theta} = \frac{1}{4}$, i.e.

$$\cos^2\bar{\theta} = 1 - \frac{1}{4n^2}. \tag{6.5}$$

Therefore, the corresponding exponential solutions have growth rate $\sigma = \delta|b(n, \bar{\theta}, \phi)|$ that is, from (6.2) and (6.5):

$$\sigma = \tfrac{1}{4}\delta\left(1 - \frac{1}{4n^2}\right)|\cos 2\phi|.$$

Subharmonic resonance is then maximized when $\phi = 0$, π or $\pm\frac{1}{2}\pi$, i.e. when the horizontal projection of the wave vector $\boldsymbol{k}_h$ is aligned with one of the principal axes of strain. The maximum growth rate (over θ and ϕ) thus reads (in t^* units):

$$\sigma = \tfrac{1}{4}\delta\left(1 - \frac{1}{4n^2}\right). \tag{6.6}$$

Remember that this is precisely the case where the assumption of zero vertical vorticity perturbation ($\eta = 0$) is not required†.

The maximum growth rate given by (6.6) grows monotonously with n, from 0 for for $n = \frac{1}{2}$ to $\frac{1}{4}\delta$ when $n \to \infty$, which means that resonance persists for any strong

† In the presence of the inhomogeneous term when $\eta \neq 0$, system (3.3b) and (4.3) reduces for small δ to the Mathieu equation (6.1) with harmonic forcing $\delta K \sin t^*/\sin^4\theta$ on its right-hand side. It may be shown by multiple scale asymptotics that only the second-order resonance is affected by the forcing term, the leading-order subharmonic resonance being unaffected. Therefore, vertical vorticity has negligibly small effects on the results for weak strain.

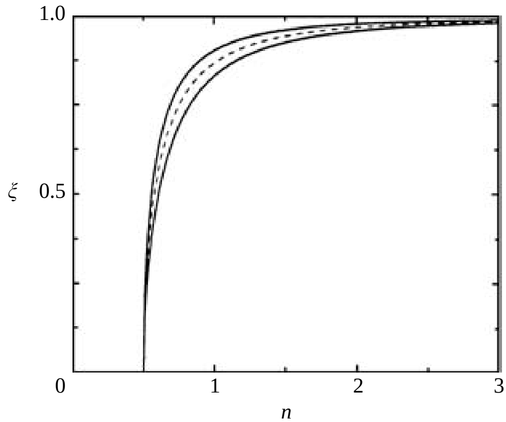

FIGURE 3. Initial orientation $\xi = \cos\theta$ of the wave vector with the z-axis, for subharmonic resonance and $\phi = 0$ in the asymptotic regime $\delta \ll 1$, as a function of the frequency ratio $n = N/\omega$. The dashed line given by (6.5) corresponds to the initial angle $\bar{\theta}$ for maximum instability. The solid lines are the boundaries of the unstable region $\cos\theta_{\pm}$ defined in (6.7) and plotted here for $\delta = \frac{1}{3}$.

stratification. In the latter case, (6.5) tells us that the orientation of the resonant wave vector tends to be aligned with the vertical direction. However, we have seen previously that modes with vertical wave vector are stable; this apparent paradox may be explained by the fact that the width of the unstable region shrinks to zero for large n. Indeed, for fixed small δ, it is not difficult to show that the unstable region defined by (6.4) for the Mathieu equation corresponds to an interval $\theta_- < \theta < \theta_+$ where $\theta_{\pm}$ are defined by

$$\cos^2\theta_{\pm} = \left(1 - \frac{1}{4n^2}\right)\left(1 \mp \frac{\delta}{4n^2}\right), \tag{6.7}$$

in which exponential growth occurs. Clearly, the width of this interval shrinks for large stratification. This is illustrated in figure 3.

Let us summarize the results of this section: for weak amplitudes $\delta \ll 1$ of the background strain field, internal gravity waves are parametrically excited as soon as $n > \frac{1}{2}$. The most amplified waves have a wave vector which lies either in the (x, z) or in the (y, z)-plane, with initial angle $\bar{\theta}$ with the vertical direction given by (6.5), and maximum growth rate σ (in t^* units) given by (6.6). Let us now examine the case of large amplitudes.

7. Higher-order resonances; numerical computations

For large amplitudes δ of the background strain field, the temporal behaviour of the solutions may be obtained by integrating over one period 2π the fundamental matrix solution $\mathscr{P}$ associated with Hill's equation (5.2):

$$\frac{\mathrm{d}\mathscr{P}}{\mathrm{d}t^*} = \begin{pmatrix} 0 & 1 \\ -n^2\dfrac{|\boldsymbol{k}_h(t^*)|^2}{|\boldsymbol{k}(t^*)|^2} & 0 \end{pmatrix}\mathscr{P}, \quad \mathscr{P}(0) = \mathscr{I}, \tag{7.1}$$

and by computing the eigenvalues of the monodromy matrix $\mathscr{M} = \mathscr{P}(2\pi)$ thus obtained. They are roots of the following characteristic equation (Cesari 1959):

$$\lambda^2 - \lambda \mathrm{tr}(\mathscr{M}) + 1 = 0.$$

Exponential growth occurs if and only if $|\mathrm{tr}(\mathscr{M})| > 2$ with growth rate

$$\sigma = \frac{\log \lambda}{2\pi},$$

$\lambda > 1$ being the largest root of the characteristic equation (the other one being $1/\lambda < 1$). This procedure, which essentially follows Floquet's theory, has been introduced by Bayly (1986) in the field of hydrodynamic stability theory.

System (7.1) has been integrated numerically over one period using a fourth-order Runge–Kutta scheme with 10^{-3} time step, for various values of the parameters

$$n > \tfrac{1}{2}, \quad 0 \leqslant \delta < 1, \quad 0 \leqslant \theta < \tfrac{1}{2}\pi, \quad 0 \leqslant \phi \leqslant \tfrac{1}{4}\pi.$$

In each case, it was found that subharmonic resonance was maximized when $\phi = 0$, as already observed in the previous section for $\delta \ll 1$, so that the results given below only correspond to that case.

Typical numerical results are plotted in figures 4 and 5. Cases (*a*), (*b*) and (*c*) correspond, respectively, to particular values of n satisfying $n > \frac{1}{2}j$, with $j = 1, 2$ and 3, respectively, so that subharmonic ($j = 1$) resonance is expected in each case, fundamental ($j = 2$) in cases (*b*) and (*c*), and superharmonic ($j = 3$) in case (*c*). Each resonance tongue reaches the axis $\delta = 0$ at an angle θ_j defined by:

$$\cos^2\theta_j = 1 - \frac{j^2}{4n^2} \quad (j = 1, 2, 3, \cdots). \tag{7.2}$$

This is clearly illustrated in figure 4, where the values of n have been chosen so that the highest-order resonance arises from the axis $\delta = 0$ at $\cos\theta_j = \frac{1}{2}$. As expected, the most unstable resonance remains the subharmonic one, as illustrated in figure 5 where the results are compared to weak strain asymptotics with rather good agreement.

Figure 6 presents another view of the first three tongues of resonance, for a moderate amplitude of strain: $\delta = \frac{1}{2}$. All three are centred around the curves given by (7.2), emanating from the axis $\xi = 0$ at $n = \frac{1}{2}j$ for $j = 1, 2$ and 3. Again, the subharmonic resonance is the most amplified, and the width of its tongue decreases as n increases, as expected from asymptotics (figure 3). On the other hand, stability holds for $n \leqslant \frac{1}{2}$ in agreement with Joukowski's theorem.

8. Strong stratification and self-similarity

Let us now examine in more detail the case of strong stratification $N \gg \omega$ (i.e. $n \gg 1$), of interest for modelling in geophysics. Since we have seen previously that it is the most dangerous, we will focus on the subharmonic resonance.

In the case of weak-amplitude oscillating strain $\delta \ll 1$, we found with asymptotics that the maximum growth rate (in t^* units) is given by (6.6), so that:

$$\lim_{n\to\infty} \sigma = \tfrac{1}{4}\delta. \tag{8.1}$$

The interesting point is that growth rate becomes independent of n. Furthermore, we recall that the maximum growth rate (6.6) corresponds to perturbations for which the angle $\bar{\theta}$ of the wave vector with the vertical axis satisfies the condition $n^2 \sin^2\bar{\theta} = \frac{1}{4}$ for

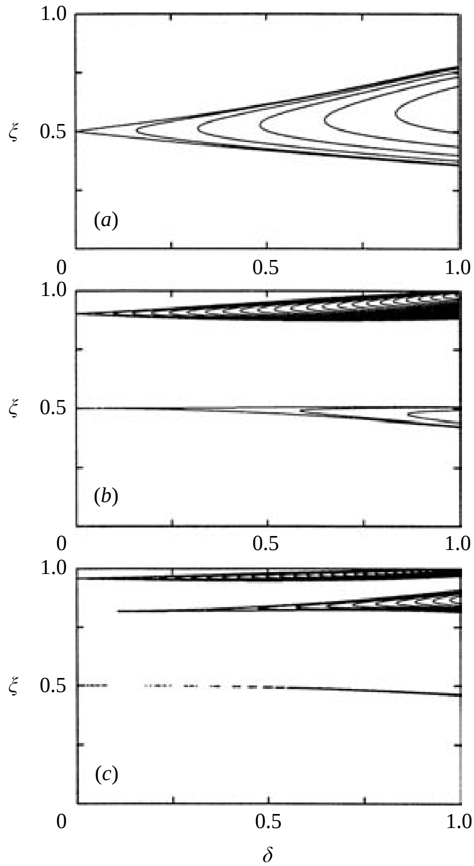

FIGURE 4. Contour lines for the growth rate σ of perturbations with $\phi = 0$, as a function of the amplitude δ of the background strain and the initial orientation $\xi = \cos\theta$ of the wave vector, for different values of the frequency ratio $n = N/\omega$: (a) $n = \frac{1}{3}\sqrt{3}$ ($\approx$0.577); (b) $n = \frac{2}{3}\sqrt{3}$ ($\approx$1.155); (c) $n = \sqrt{3}$ ($\approx$1.732). Contour lines are plotted from 10^{-10} with increments of 10^{-2}.

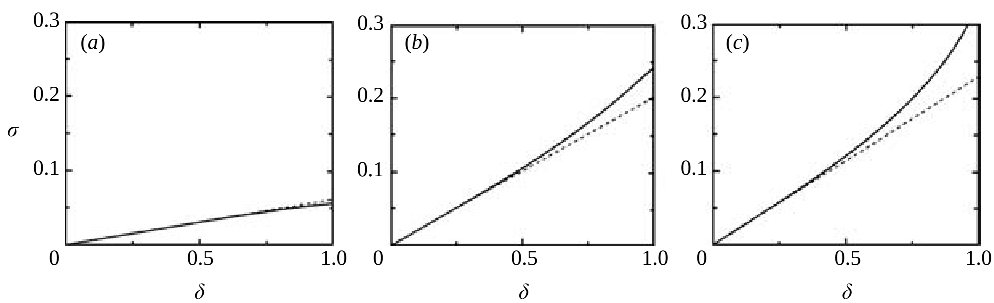

FIGURE 5. Growth rate σ maximized over θ of perturbations with $\phi = 0$, as a function of δ and n: (a) $n = \frac{1}{3}\sqrt{3}$; (b) $n = \frac{2}{3}\sqrt{3}$; (c) $n = \sqrt{3}$. —, numerical computations; ---, asymptotics (6.6).

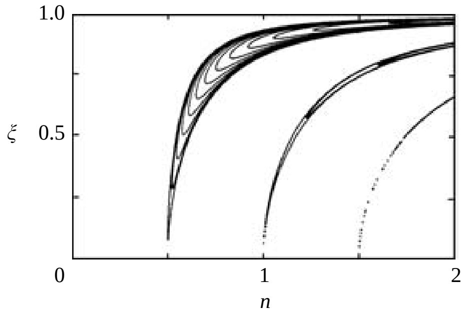

FIGURE 6. Contour lines for the growth rate σ of perturbations with $\phi = 0$, as a function of the frequency ratio $n = N/\omega$ and the initial orientation $\xi = \cos\theta$ of the wave vector, for strain amplitude $\delta = \frac{1}{2}$. Contour lines are plotted from 10^{-10} with increments of 10^{-2}.

subharmonic resonance, see (6.5). Therefore, if $n^2 \gg 1$, it is clear that this resonance condition may be ensured whenever $\bar{\theta} \ll 1$, so that $\sin\bar{\theta} = \bar{\theta}$ at first order, leading to:

$$\lim_{n\to\infty} 2n\bar{\theta} = 1. \tag{8.2}$$

Thus, the wave vector of resonant waves tends to be aligned with the vertical axis when $n \to \infty$, but its orientation angle satisfies the self-similar behaviour described in (8.2), for sufficiently strong stratification. The width of the subharmonic tongue given by (6.7) and plotted in figure 3 is also self-similar for large n. Indeed, developing the right-hand side of (6.7), neglecting the term of order n^{-4}, and transforming the cosine into sine, we obtain $4n^2\sin^2\theta_\pm = 1 \pm \delta$, so that, by an argument similar to that for $\bar{\theta}$, we obtain for $\theta_\pm$,

$$\lim_{n\to\infty} 2n\theta_\pm = 1 \pm \tfrac{1}{2}\delta. \tag{8.3}$$

for any sufficiently small δ.

To summarize, for weak strain and large stratification, asymptotics tells us that:

(i) Subharmonic resonance occurs when $1 - \frac{1}{2}\delta < 2n\theta < 1 + \frac{1}{2}\delta$;
(ii) The most unstable mode is such that $2n\bar{\theta} = 1$;
(iii) Its growth rate is given by $\sigma = \frac{1}{4}\delta$.

This is illustrated in figure 7 where the rescaled initial angles corresponding to maximum instability $2n\bar{\theta}$ and to resonance boundaries $2n\theta_\pm$ are plotted as a function of n, computed, respectively, from (6.5) and (6.7). It shows clearly that for sufficiently large (even moderate) values of n, the curves become independent of n and the asymptotic values agree well with (8.2) and (8.3). Therefore, figure 7, which is merely a rescaled plot of figure 3 (with a smaller δ, however), exhibits clearly the self-similarity of the resonant mechanism.

When δ is not small (large strain), asymptotic results are no longer available, however, we observe by numerical computations qualitatively the same features as for weak strain. The only difference is that when $n \to \infty$, the asymptotic values in (8.1), (8.2) and (8.3) now depend nonlinearly on the strain amplitude δ. However, for fixed δ, the important point remains that these values are independent of n. This is illustrated in figure 8 which plots the subharmonic tongue for $\delta = \frac{1}{2}$ in terms of the rescaled angle $2n\theta$. This has to be compared with figure 6 where we recall that

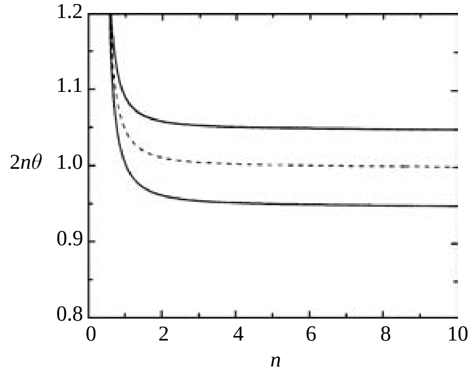

FIGURE 7. Rescaled initial orientation $2n\theta$ of the wave vector for subharmonic resonance with $\phi = 0$ in the asymptotic regime $\delta \ll 1$, as a function of the frequency ratio $n = N/\omega$. The dashed line corresponds to the angle $\bar{\theta}$ for maximum instability, calculated from (6.5). Solid lines correspond to the boundaries of the unstable region $\theta_{\pm}$ computed from (6.7) and plotted here for $\delta = \frac{1}{10}$.

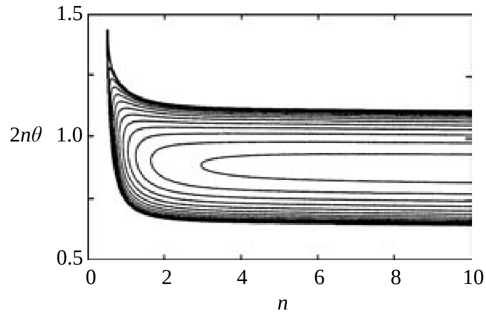

FIGURE 8. Contour lines for the growth rate σ of subharmonic resonance, as a function of the frequency ratio $n = N/\omega$ and the rescaled initial orientation $2n\theta$ of the wave vector, with $\phi = 0$. Strain amplitude is $\delta = \frac{1}{2}$. Contour lines are plotted from 10^{-10} with increments of 10^{-2}.

subharmonic resonance starts at $n = \frac{1}{2}$. Again, the signature of self-similarity is that the contour lines of the growth rate are horizontal for sufficiently large n.

9. The Billant–Chomaz scaling

In fact, the previous analysis has been motivated by the work of Billant & Chomaz (2001) who, in the light of their results on zigzag instability (Billant & Chomaz 2000*a–c*), discovered a new scaling for strongly stratified flows taking into account rapid vertical variations. In the inviscid case, they pointed out that the resulting dimensionless Boussinesq equations reduce to a set of equations that are not two-dimensional, as previously stated (see for instance Riley & Lelong 2000), but in which only the vertical acceleration is neglected. Furthermore, these reduced equations are self-similar with respect to the rescaled vertical coordinate. We shall now prove that the mechanism of resonance exposed in the present paper may be described by these reduced dynamics, and that the Billant–Chomaz self-similarity law corresponds in fact to that pointed out in the previous section.

Following Billant & Chomaz (2001), we first write the governing equations in dimensionless form. Instead of starting from the Eulerian perturbation equations (2.4), we consider system (3.3) which involves no more space derivatives, but the wave vector $\boldsymbol{k}$. The small parameter defined by the ratio between the vertical and horizontal length scales which is the key point of the Billant–Chomaz scaling, is replaced here by the initial wave vector angle giving rise to parametric resonance. This is natural since our problem involves no spatial scale. Let ω^{-1} be the characteristic advective time scale. The ratio $\omega/N = 1/n$ thus defines a Froude number, analogous to the horizontal Froude number F_h defined in Billant & Chomaz (2001). Let U be a characteristic horizontal velocity scale, we introduce:

$$t = t^*/\omega, \quad \mathscr{S}_h = \omega \mathscr{S}_h^*, \quad \varpi = U^2 \varpi^*, \quad q = UNq^*,$$

where the dimensionless variables noted with a star depend on the rescaled time t^*. The dimensionless velocity perturbation $\boldsymbol{v}^* = \boldsymbol{v}_h^* + w^* \boldsymbol{e}_z$ and wave vector $\boldsymbol{k}^* = \boldsymbol{k}_h^* + \xi^* \boldsymbol{e}_z$ are defined by:

$$\boldsymbol{v}_h = U \boldsymbol{v}_h^*, \quad w = \frac{\omega U}{N} w^*, \quad \boldsymbol{k}_h = \frac{\omega}{U} \boldsymbol{k}_h^*, \quad \xi = \frac{N}{U} \xi^*, \tag{9.1}$$

to take into account both weakness of the vertical velocity in strongly stratified flows, and its rapid variations in the vertical direction. With these scalings, system (3.3) reads in dimensionless form:

$$\frac{\mathrm{d}\boldsymbol{v}_h^*}{\mathrm{d}t^*} + \mathscr{S}_h^* \boldsymbol{v}_h^* + \mathrm{i}\boldsymbol{k}_h^* \varpi^* = 0, \tag{9.2a}$$

$$\frac{1}{n^2} \frac{\mathrm{d}w^*}{\mathrm{d}t^*} + \mathrm{i}\xi^* \varpi^* = q^*, \tag{9.2b}$$

$$\frac{\mathrm{d}q^*}{\mathrm{d}t^*} + w^* = 0, \tag{9.2c}$$

together with $\boldsymbol{k}^* \cdot \boldsymbol{v}^* = 0$. When $n \to \infty$, we obtain at first order a system of equations where only the vertical acceleration is neglected from the initial Boussinesq; this is the Billant–Chomaz reduced dynamics.

We shall show now that it describes accurately the physics of our problem, when stratification is strong. Dropping the term of order n^{-2} in (9.2*b*), the system above may be reduced to a single Hill equation in a straightforward manner. Introducing the new variable p^* defined by:

$$p^* = \frac{\xi^{*2}}{|\boldsymbol{k}_h^*|^2} w^*,$$

we obtain (for zero vertical vorticity):

$$\frac{\mathrm{d}^2 p^*}{\mathrm{d}t^{*2}} + \frac{|\boldsymbol{k}_h^*(t^*)|^2}{\xi^{*2}} p^* = 0. \tag{9.3}$$

Remembering that from (3.2), in dimensional form:

$$\frac{|\boldsymbol{k}_h(t)|^2}{\xi^2} = \tan^2\theta \left(\frac{\cos^2\phi}{R^2(t)} + R^2(t)\sin^2\phi \right),$$

the term in parentheses being of order unity, the only way for $|\boldsymbol{k}_h|^2/\xi^2$ to be of order n^{-2}, as expected from scaling (9.1), is for $\tan^2\theta$ to be of order n^{-2}. Thus, if we set:

$$\theta^* = 2n\theta,$$

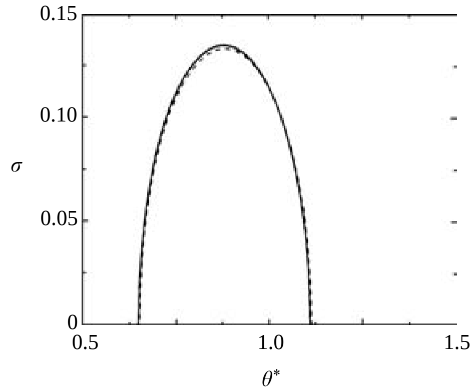

FIGURE 9. Growth rate σ of subharmonic resonance as a function of the similarity parameter $\theta^* = 2n\theta$ for modes with $\phi = 0$. Comparison between the Billant–Chomaz reduced dynamics (solid line) and the full dynamics with $n = 5$ (dashed line). Strain amplitude is $\delta = \frac{1}{2}$.

with θ^* of order one (the factor 2 is introduced for convenience), we obtain in dimensionless form:

$$\frac{|\boldsymbol{k}_h^*(t^*)|^2}{\xi^{*2}} = \frac{\theta^{*2}}{4}\left(\frac{\cos^2\phi}{R^2(t^*)} + R^2(t^*)\sin^2\phi\right), \tag{9.4}$$

where $R(t^*) = 1+\delta\sin t^*$. Together with (9.3), this is the Hill's equation corresponding to the Billant–Chomaz reduced dynamics, i.e. to system (9.2) at zeroth order. Note that (9.3) could have been obtained directly from (4.5), but we have preferred to rederive it from the original system to emphasize the analogy with the Billant–Chomaz scaling.

As previously mentioned, the most interesting cases correspond to $\phi = 0$, π or $\pm\frac{1}{2}\pi$ on which we focus our attention. Also, when $\delta \ll 1$ and $\phi = 0$ in (9.4), we obtain immediately the following Mathieu equation:

$$\frac{\mathrm{d}^2 p^*}{\mathrm{d}t^{*2}} + \frac{\theta^{*2}}{4}(1 - 2\delta\sin t^*)p^* = 0,$$

for which subharmonic instability arises when $1 - \delta < \theta^{*2} < 1 + \delta$, the maximum growth rate $\sigma = \frac{1}{4}\delta$ being reached for $\theta^* = 1$. Since $\theta^* = 2n\theta$, we recover the asymptotic results obtained in the previous section for $n \to \infty$, see items (i)–(iii).

For larger amplitudes of strain, comparisons between the computed solutions of the reduced Hill equation, (9.3), and the full equation, (5.2), for sufficiently large stratification parameter n are in excellent agreement. For $\delta = \frac{1}{2}$, growth rate of subharmonic resonance is plotted in figure 9 versus the similarity parameter $\theta^* = 2n\theta$. Even for moderate stratification ($n = 5$), the curves are nearly the same and higher values of n (for instance $n = 10$) have not been plotted since they are confused with the results of reduced dynamics. This means self-similarity is nearly reached for $n = 5$, and is achieved for $n \geqslant 10$, as was expected from figures 7 and 8.

As a conclusion of this section, the reduced dynamics suggested by Billant & Chomaz (2001) describes accurately the physics of the present instability mechanism, as soon as stratification is strong enough. Before summarizing the results of the paper and discussing layer formation, let us say a few words on the effects of viscosity on parametric instabilities.

10. Viscous damping

In the presence of diffusion, system (3.3) is replaced by (see Craik 1989):

$$\dot{\boldsymbol{v}} + \mathscr{S}\boldsymbol{v} + \mathrm{i}\boldsymbol{k}\varpi = q\boldsymbol{e}_z - \nu|\boldsymbol{k}|^2\boldsymbol{v},$$
$$\dot{q} + N^2\boldsymbol{v}\cdot\boldsymbol{e}_z = -\kappa|\boldsymbol{k}|^2 b,$$
$$\boldsymbol{k}\cdot\boldsymbol{v} = 0,$$

where ν is the kinematic viscosity, and κ is either the heat conductivity (Majda & Shefter 1998) or the molecular diffusivity of the stratifying agent (Billant & Chomaz 2000*a–c*). The ratio ν/κ thus defines either a Prandtl or a Schmidt number. Two situations are examined below: $\nu/\kappa = 1$ which is exactly tractable mathematically, and $\nu/\kappa \gg 1$ which is physically more realistic (see for instance discussions in Majda & Shefter 1998; Billant & Chomaz 2000*a–c*).

The vertical vorticity perturbation governed by $\dot{\eta} = -\nu|\boldsymbol{k}|^2\eta$ reads:

$$\eta(t) = \eta(0)\exp\left(-\nu\int_0^t |\boldsymbol{k}(s)|^2\,\mathrm{d}s\right),$$

so that $|\eta|$ may be bounded from above by an exponentially decreasing function of time, since $|\boldsymbol{k}|^2$ is bounded; therefore, the vertical vorticity perturbation decreases to zero for any small amount of viscosity, as anticipated in the beginning of the paper. Thus, once again, we assume $\eta(0) = 0$. System (4.4) is then replaced by:

$$\left(\frac{\mathrm{d}}{\mathrm{d}t} + \nu|\boldsymbol{k}|^2\right)p = q, \quad \left(\frac{\mathrm{d}}{\mathrm{d}t} + \kappa|\boldsymbol{k}|^2\right)q = -N^2\frac{|\boldsymbol{k}_h|^2}{|\boldsymbol{k}|^2}p. \tag{10.1}$$

The standard transformation used in non-stratified flows (Lagnado *et al.* 1984; Craik 1989) is not valid here, except in the exceptional case where $\nu = \kappa$ which may be treated in closed form. In that case, introducing the following change of variables:

$$p(t) = \bar{p}(t)\exp\left(-\nu\int_0^t |\boldsymbol{k}(s)|^2\,\mathrm{d}s\right),$$

and the same for buoyancy q, the new variable $\bar{p}$ is governed by the inviscid homogeneous Hill's equation (4.5). The wave vector being periodic then bounded in time, it is clear that inviscid resonances will either be damped or eventually suppressed by diffusion.

Turning now to the more realistic case where the Prandtl number is large, i.e. $\kappa \ll \nu$, and even neglecting heat conduction $\kappa = 0$ (a value for which we are happy to recover mass conservation), system (10.1) reduces to the equation:

$$\frac{\mathrm{d}^2p}{\mathrm{d}t^2} + \nu|\boldsymbol{k}|^2\frac{\mathrm{d}p}{\mathrm{d}t} + \left(N^2\frac{|\boldsymbol{k}_h|^2}{|\boldsymbol{k}|^2} - 2\nu\boldsymbol{k}_h\cdot\mathscr{S}_h\boldsymbol{k}_h\right)p = 0, \tag{10.2}$$

which may be put in Hill's form using a complicated transformation (Cesari 1959). Analysis is more tractable when both strain and viscosity are weak, i.e. $\nu = \delta\bar{\nu}$ with $\delta \ll 1$ and $\bar{\nu}$ of order one. In that case, indeed, (10.2) reduces to the weakly damped Mathieu equation (with rescaled time $t^* = \omega t$):

$$\frac{\mathrm{d}^2p}{\mathrm{d}t^{*2}} + 2\delta\lambda\frac{\mathrm{d}p}{\mathrm{d}t^*} + (a + 2\delta b\sin t^*)p = 0,$$

where $a(n, \theta)$ and $b(n, \theta, \phi)$ are still given in (6.2), and

$$\lambda = \frac{\bar{\nu} k_0^2}{2\omega}.$$

We see here the appearance of the initial magnitude k_0 of the wave vector, inessential in the inviscid case. On introducing the new variable $\bar{p}$ defined by:

$$p(t^*) = \bar{p}(t^*)\mathrm{e}^{-\delta\lambda t^*},$$

and neglecting terms of order δ^2, we obtain the inviscid Mathieu equation (6.1) for $\bar{p}$. As a consequence, we immediately conclude that the viscous growth rate (in t^* units) of subharmonic resonance is $\sigma - \delta\lambda$, the maximum inviscid growth rate σ being given in (6.6) in the limit of small amplitude of strain.

Transition between stability and subharmonic resonance is then shifted to

$$n = \frac{1}{2\sqrt{1 - 4\lambda}},$$

instead of $n = \frac{1}{2}$ in the inviscid case. Therefore, when $\lambda \leqslant \frac{1}{4}$, i.e. $\nu k_0^2 \leqslant \frac{1}{2}\delta\omega$, viscosity deletes parametric instability.

11. Discussion

Let us summarize the main results of the paper. A stably stratified flow with Brunt–Väisälä frequency N stretched time-periodically with positive frequency ω in the horizontal plane is stable when $N \leqslant \frac{1}{2}\omega$ and unstable otherwise. Three-dimensional instability results from a mechanism of parametric excitation of internal gravity waves leading to exponential growth of their amplitude. The most amplified resonance is subharmonic and corresponds to the wave vector whose angle with the vertical axis θ satisfies:

$$N \sin\theta = \tfrac{1}{2}\omega,$$

so that for strong stratification $N \gg \omega$, the waves that are resonantly excited by strain are those whose wave vector is nearly aligned with the z-axis, nearly but not completely since resonance is impossible when $\theta = 0$. Furthermore, since $\omega_0 = \pm N \sin\theta$ is the frequency of undisturbed internal waves propagating in a uniform medium at rest (with $0 \leqslant |\omega_0| \leqslant N$), we then see that the resonant waves are the slow ones since their frequency $|\omega_0| = \frac{1}{2}\omega$ is much weaker than N for large stratification.

In the light of the work of Billant & Chomaz (2001), some interesting properties of these parametric instabilities have also been identified. Indeed, when stratification is strong enough, that is $N \gg \omega$ with fixed ω, the growth rate of subharmonic resonant waves is (in dimensional time units) $\frac{1}{4}\delta\omega$, for sufficiently small strain amplitude δ, so that the growth rate does not depend on N. Furthermore, the wave vector angle θ for which the wave grows exponentially is such that:

$$N\theta = \tfrac{1}{2}\omega,$$

so that for strong stratification, the mechanism of resonance becomes self-similar with respect to the parameter $\theta N/\omega$. Since θ is the angle between the disturbance wave vector ($\boldsymbol{k} = \boldsymbol{k}_h + \xi \boldsymbol{e}_z$) and the z-axis, this means that $\xi/|\boldsymbol{k}_h|$ is of order N, so that in physical space, variations in the vertical directions are much more rapid than in the horizontal directions. This is precisely the basis of the Billant–Chomaz scaling, leading to dimensionless Boussinesq equations in which only the vertical acceleration is dropped for infinite stratification. The resulting equations are self-similar with respect to zN/U (where U is a characteristic horizontal velocity scale), which has the same physical significance as our similarity parameter $\theta N/\omega$. Both our asymptotic and numerical results have shown that the reduced dynamics suggested by Billant & Chomaz (2001) describe accurately the behaviour of the full solution in the limit of infinite stratification.

By contrast, since parametric instabilities described in the present paper are three-dimensional, it is clear that the usual scaling for strongly stratified flows (Riley & Lelong 2000) is inadequate here, since it leads at leading order to two-dimensional dynamics in horizontal planes, with arbitrary vertical dependence for the horizontal velocity in the inviscid case†.

As noted earlier, the wave vector $\boldsymbol{k}$ of resonant waves is nearly aligned with the z-axis for strong stratification and weak strain. Therefore, since $\boldsymbol{k}\cdot\boldsymbol{v} = 0$ and $\boldsymbol{k}\cdot\boldsymbol{\omega} = 0$, both velocity and vorticity perturbations grow exponentially nearly horizontally, promoting the formation of correlated quasi-horizontal layers with high vertical shear. It is worth noting that our conclusions are similar to those of Billant & Chomaz (2000*a*–*c*). Indeed, although the underlying physical mechanisms are clearly different from those exposed in the present study, their zigzag instability which develops in dipolar vortices is self-similar for strong stratification, and also promotes layering. As a consequence, various alternative mechanisms may be involved to explain the early stage of layer formation. This is not surprising since these horizontal layers, that are so commonly observed in strongly stratified flows, might be interpreted as an attractor for the solutions of the Boussinesq equations. This is an open question, but the scaling of Billant & Chomaz (2001) supports this conjecture.

Closely related to this topic, rapid distortion theory of homogeneous stratified turbulence provides a first natural extension of our study since it is well known that the mathematical basis is the same: uniform strain flow and plane waves (see Cambon & Scott 1999). In that context, our problem would correspond to a homogeneous turbulent field in statistical equilibrium, periodically distorted by a large-scale horizontal strain field, leading to the exponential growth of small-scale three-dimensional fluctuations. With a stochastic instead of periodic temporal law for the strain field, this might mimic the numerical experiments of forced stratified turbulence (Herring & Métais 1989; Smith & Waleffe 2002). This is currently under investigation.

Another perspective of the present work would be the study of secondary perturbations to the flow consisting of periodic strain field plus plane wave solutions, both in the stable and resonant cases. Without strain field, finite-amplitude internal gravity waves are known to be unstable in an unbounded domain, as explained in the pioneering works of Mied (1976) and Drazin (1977), and observed experimentally by Benielli & Sommeria (1998) with external excitation. In the presence of strain, the stability analysis of resonant internal waves might be performed in the fashion of Fabijonas, Holm & Lifschitz (1997) for secondary perturbations of elliptical flows.

Of course, an experimental verification of our results would be welcome, such as inside an elastic cylinder. Qualitatively, we think that the experiments would follow the main results of the paper. However, in order to compare with theory more closely,

† In the viscous case, however, the reduced dynamics resulting from the scaling given in Riley & Lelong (2000) is no longer two-dimensional, but involves an exchange of momentum through vertical diffusion, which may lead to the reorganization of the flow into layers, as demonstrated by Majda & Grote (1997).

much work remains to be done. Indeed, the inviscid results presented in the paper may be directly applied to the bounded flow inside an elastic cylinder, by considering plane wave solutions as short-wave perturbations (see for instance Friedlander & Vishik 1991; Bayly *et al.* 1996; Fabijonas *et al.* 1997; Leblanc 1997; Le Dizès 2000) this approach is known to give the correct asymptotic behaviour for discrete modes with large wavenumbers. Viscosity, however, selects modes with moderate wavenumbers, so that the stability of a bounded flow generally requires an eigenmode analysis to capture complementary information on discrete modes (for the elliptical instability, see for instance Waleffe 1990; Gledzer & Ponomarev 1992). Furthermore, each plane wave perturbation being an exact nonlinear solution in the unbounded case even in a stratified flow thanks to incompressibility (Bayly 1986; Craik 1989), it is clear that boundedness will imply non-trivial nonlinear effects, as for the elliptical instability (see Kerswell 2002). As a consequence, a weakly nonlinear analysis including viscosity and boundaries might be useful.

Before tackling this program, we conclude this work by a related topic for which Joukowski's theorem may be applied: the elliptical instability.

12. Epilogue. The elliptical instability in a rotating stratified flow

The theory of the paper may be applied to the stability of a uniform elliptic vortex in a stably stratified rotating flow, when relative vorticity, background rotation and gravity are all parallel to the z-axis, say. Indeed, in a relative frame rotating with constant angular velocity $\boldsymbol{\Omega} = \Omega \boldsymbol{e}_z$, let

$$\mathscr{L}^{(r)} = \begin{pmatrix} 0 & -\frac{1}{2}W - S & 0 \\ \frac{1}{2}W - S & 0 & 0 \\ 0 & 0 & 0 \end{pmatrix},$$

be the uniform velocity gradient of a steady uniform elliptical flow with relative vorticity W and strain rate S, where $0 < S < \frac{1}{2}W$ so that streamlines are ellipses. By composition of velocities, it is easy to show that the absolute velocity field of the flow under consideration has a spatially uniform gradient $\mathscr{L}^{(a)} = \mathscr{S}^{(a)} + \mathscr{A}^{(a)}$ where

$$\mathscr{S}^{(a)}(t) = \begin{pmatrix} S\sin(2\Omega t) & -S\cos(2\Omega t) & 0 \\ -S\cos(2\Omega t) & -S\sin(2\Omega t) & 0 \\ 0 & 0 & 0 \end{pmatrix}, \tag{12.1}$$

is the symmetric part which corresponds to a rotating strain field, and

$$\mathscr{A}^{(a)} = \begin{pmatrix} 0 & -\frac{1}{2}(W + 2\Omega) & 0 \\ \frac{1}{2}(W + 2\Omega) & 0 & 0 \\ 0 & 0 & 0 \end{pmatrix},$$

is the skew symmetric part involving the absolute vorticity $W + 2\Omega$ which plays an important role in geophysical flows (see for instance LeBlond & Mysak 1978). This is the vorticity of the flow viewed from the absolute frame.

In the case where background rotation counterbalances the intrinsic rotation of the elliptical vortex, i.e. at zero absolute vorticity:

$$W + 2\Omega = 0,$$

the flow under consideration is irrotational in the inertial frame, and the velocity gradient $\mathscr{L}^{(a)}$ of the absolute velocity field is reduced to the time-periodic symmetric strain tensor $\mathscr{S}^{(a)}$. Therefore, the theory of the present paper may be applied to derive the following result.

COROLLARY 2. *In a rotating stratified flow, the elliptical vortex is stable at zero absolute vorticity when:*

$$N^2 \leqslant \tfrac{1}{4}W^2 - S^2. \tag{12.2}$$

Indeed, as noted earlier, derivation of Hill's equation, (4.5), holds for any irrotational flow with time-periodic strain tensor, so that in the inertial frame, the stability analysis of the rotating stratified elliptical flow at zero absolute vorticity may be studied straightforwardly. By contrast to the strain flow (2.2) studied thoroughly in the paper, the period of $|\boldsymbol{k}_h|^2/|\boldsymbol{k}|^2$ involved in Hill's equation differs here from that of the strain tensor (12.1) and must be determined. Euclidean norm being invariant by any change of basis, $|\boldsymbol{k}_h|^2/|\boldsymbol{k}|^2$ may be evaluated with $\boldsymbol{k}$ expressed in either the relative or the absolute frame, the most convenient being the former. Indeed, the solution of $\dot{\boldsymbol{k}} = -\boldsymbol{k}^T\mathscr{L}^{(r)}$ may be written as (Bayly 1986; Waleffe 1990):

$$\boldsymbol{k}(t) = (k_0 \sin\theta \cos\omega t,\ k_0\mu \sin\theta \sin\omega t,\ k_0 \cos\theta)^T,$$

where

$$\omega = \sqrt{\tfrac{1}{4}W^2 - S^2}, \quad \mu = \frac{\omega}{\tfrac{1}{2}W - S}.$$

Therefore, $|\boldsymbol{k}_h|^2/|\boldsymbol{k}|^2$ is time-periodic with period π/ω, so that application of Joukowski's theorem with $j = 0$ concludes the proof.

Without stratification, it is now well known that an elliptical flow at zero absolute vorticity is stable for any ellipticity. Observed numerically by Craik (1989), this result has been proved by Cambon *et al.* (1994) and revisited in Leblanc (1997). Stratification therefore affects this picture, and (12.2) even suggests instability at zero absolute vorticity for sufficiently strong stratification. This will be confirmed below in the asymptotic limit of weak strain.

It is also worth noting that condition (12.2) contrasts with an observation made by Miyazaki & Fukumoto (1992) concerning the elliptical stratified flow without rotation. Recall that in a homogeneous non-rotating flow, elliptical instability corresponds to the subharmonic resonance of the corresponding Hill (or Mathieu) equation (Waleffe 1990); Miyazaki & Fukumoto (1992) found numerically that this subharmonic resonance is suppressed when

$$N^2 \geqslant \tfrac{1}{4}W^2 - S^2, \tag{12.3}$$

for $\Omega = 0$, but observed the emergence of higher-order resonances for any strong stratification, although with weaker growth rate. As a consequence, (12.3) is not a sufficient condition for stability, contrary to (12.2).

Thus, we see that the combined effects of rotation and stratification on the stability of the elliptical vortex are subtle. This problem has been addressed briefly by Gledzer & Ponomarev (1992), and an overall picture has been drawn by Miyazaki (1993) with numerical computations. However, a systematic asymptotic analysis in the case of weak ellipticity was lacking. This point has been addressed briefly in Kerswell (2002). Some further explanations may be noteworthy, at least to distinguish clearly stable to unstable regions in the (Ω, N) parameter plane.

Let us introduce the following dimensionless quantities:

$$\delta = 2S/W, \quad f = 2\Omega/W, \quad n = N/W,$$

and assume that strain is weak: $\delta \ll 1$. After lengthy calculations that we do not detail here, the stability problem is once again reduced to a Mathieu equation like (6.1), where now:

$$a(f, n, \theta) = (1 + f)^2 \cos^2\theta + n^2 \sin^2\theta,$$

and

$$b(f, n, \theta) = \tfrac{1}{2}\left(\left((1 + f)^2 - n^2\right) \sin^2\theta + f + \tfrac{3}{2}\right) \cos^2\theta,$$

time now being normalized by the relative vorticity, i.e. $t^* = Wt$.

Parametric resonances occur when $a(f, n, \theta_j) = \frac{1}{4} j^2$ with j an integer, that is when

$$4(1 + f)^2 \cos^2\theta_j + 4n^2 \sin^2\theta_j = j^2,$$

in accordance with Miyazaki (1993)†. It is then not difficult to show that the first-order parametric resonance (the subharmonic one $j = 1$) develops for angles θ in the vicinity of $\bar{\theta}$ such that:

$$\cos^2\bar{\theta} = \frac{1 - 4n^2}{4((1 + f)^2 - n^2)}, \tag{12.4}$$

so that exponential instability occurs either when

$$n^2 \leqslant \tfrac{1}{4} \leqslant (1 + f)^2, \tag{12.5}$$

or when

$$(1 + f)^2 \leqslant \tfrac{1}{4} \leqslant n^2. \tag{12.6}$$

Growth rate (in t^* units) is:

$$\sigma = \frac{\delta}{32} \frac{(3 + 2f)^2(1 - 4n^2)}{(1 + f)^2 - n^2}, \tag{12.7}$$

in accordance with Kerswell (2002), which generalizes the asymptotic growth rates calculated successively by Waleffe (1990), Miyazaki & Fukumoto (1992) and Le Dizès (2000).

Instability conditions (12.5) and (12.6) are important because they define stable and unstable windows in the (f, n)-plane, in the asymptotic limit of weak ellipticity for subharmonic resonance. They are represented on figure 10 where the contour lines for the growth rate have been plotted. Note that stable regions at zero absolute vorticity $f = -1$ and without external rotation $f = 0$ agree, respectively, with conditions (12.2) and (12.3) when $\delta \ll 1$.

As pointed out by an anonymous referee, it should be noted that instability conditions (12.5) and (12.6) agree with Miyazaki (1993) who observed that (with our notation): 'The instability of the order lower than Min$[2n, 2|1 + f|]$ is inhibited'. In particular, when $n < \frac{1}{2}$ and $|1 + f| < \frac{1}{2}$, this tells us that not only the subharmonic

† In Miyazaki (1993), Ro corresponds to f, and N to $2n$.

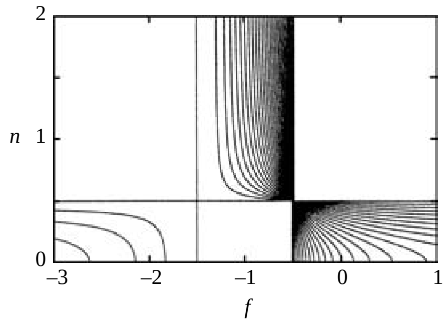

FIGURE 10. Contour lines for the rescaled growth rate σ/δ given by (12.7) for the weakly elliptical vortex in a rotating stratified flow, as a function of the rotation and stratification parameters: $f = 2\Omega/W$ and $n = N/W$. Lines $f = -\frac{3}{2}$ and $n = \frac{1}{2}$ correspond to $\sigma/\delta = 0$, whereas line $f = -\frac{1}{2}$ corresponds to maximum growth rate $\sigma/\delta = \frac{1}{2}$. The increment is 2×10^{-2}.

resonance but any order resonance is killed at vanishing ellipticity. However, resonance may arise for finite-amplitude strain, as suggested by condition (12.2) for which $f = -1$, and by numerical computations presented in figure 12 of Miyazaki (1993) for which (with our notations) $f = -0.6$ and $n = 0.3$.

At last, from (12.7), the maximum growth rate $\sigma = \frac{1}{2}\delta$ of subharmonic instability is reached at $f = -\frac{1}{2}$, which corresponds to zero tilting vorticity:

$$W + 4\Omega = 0,$$

introduced by Cambon *et al.* (1994) in the non-stratified case. This is precisely the value for which the wave vector of the disturbance is vertical $\boldsymbol{k} = \boldsymbol{e}_z$, see (12.4), giving rise to velocity and vorticity perturbations lying in the (x, y)-plane thanks to incompressibility, so that vorticity is only stretched but not tilted.

This work has been carried out at *Laboratoire des Écoulements Géophysiques et Industriels* in Grenoble. I am indebted to Chantal Staquet and Jacques Verron for their kind hospitality. I also acknowledge Evgeni Ermanyuk for telling me about Joukowski's biography, Paul Billant for useful precisions on zigzag instability, Claude Cambon for his careful reading of the manuscript, and the referees for their constructive comments.

REFERENCES

BAYLY, B. J. 1986 Three-dimensional instability of elliptical flow. *Phys. Rev. Lett.* **57**, 2160–2163.

BAYLY, B. J., HOLM, D. D. & LIFSCHITZ, A. 1996 Three-dimensional stability of elliptical vortex columns in external strain flows. *Phil. Trans. R. Soc. Lond.* A **354**, 895–926.

BENDER, C. M. & ORSZAG, S. A. 1978 *Advanced Mathematical Methods for Scientists and Engineers.* McGraw-Hill.

BENIELLI, D. & SOMMERIA, J. 1998 Excitation and breaking of internal gravity waves by parametric instability. *J. Fluid Mech.* **374**, 117–144.

BILLANT, P. & CHOMAZ, J.-M. 2000*a* Experimental evidence for a new instability of a vertical columnar vortex pair in a strongly stratified fluid. *J. Fluid Mech.* **418**, 167–188.

BILLANT, P. & CHOMAZ, J.-M. 2000*b* Theoretical analysis of the zigzag instability of a vertical columnar vortex pair in a strongly stratified fluid. *J. Fluid Mech.* **419**, 29–63.

Billant, P. & Chomaz, J.-M. 2000*c* Three-dimensional stability of a vertical columnar vortex pair in a stratified fluid. *J. Fluid Mech.* **419**, 65–91.

Billant, P. & Chomaz, J.-M. 2001 Self-similarity of strongly stratified inviscid flows. *Phys. Fluids* **13**, 1645–1651.

Cambon, C., Benoît, J.-P., Shao, L. & Jacquin, L. 1994 Stability analysis and large eddy simulation of rotating turbulence with organized eddies. *J. Fluid Mech.* **278**, 175–200.

Cambon, C. & Scott, J. F. 1999 Linear and nonlinear models of anisotropic turbulence. *Annu. Rev. Fluid Mech.* **31**, 1–53.

Cesari, L. 1959 *Asymptotic Behavior and Stability Problems in Ordinary Differential Equations*. Springer.

Craik, A. D. D. 1989 The stability of unbounded two- and three-dimensional flows subject to body forces: some exact solutions. *J. Fluid Mech.* **198**, 275–292.

Craik, A. D. D. & Allen, H. R. 1992 The stability of three-dimensional time-periodic flows with spatially uniform strain rates. *J. Fluid Mech.* **234**, 613–628.

Drazin, P. G. 1977 On the instability of an internal gravity wave. *Proc. R. Soc. Lond.* A **356**, 411–432.

Fabijonas, B., Holm, D. D. & Lifschitz, A. 1997 Secondary instabilities of flows with elliptic streamlines. *Phys. Rev. Lett.* **78**, 1900–1903.

Friedlander, S. & Vishik, M. M. 1991 Instability criteria for the flow of an inviscid incompressible fluid. *Phys. Rev. Lett.* **66**, 2204–2206.

Gledzer, E. B. & Ponomarev, V. M. 1992 Instability of bounded flows with elliptical streamlines. *J. Fluid Mech.* **240**, 1–30.

Herring, J. R. & Métais, O. 1989 Numerical experiments in forced stably stratified turbulence. *J. Fluid Mech.* **202**, 97–115.

Kerswell, R. R. 2002 Elliptical instability. *Annu. Rev. Fluid Mech.* **34**, 83–113.

Lagnado, R. R., Phan-Thien, N. & Leal, L. G. 1984 The stability of two-dimensional linear flows. *Phys. Fluids* **27**, 1094–1101.

Leblanc, S. 1997 Stability of stagnation points in rotating flows. *Phys. Fluids* **9**, 3566–3569.

Leblanc, S. & Le Penven, L. 1999 Stability of periodically compressed vortices at low Mach number. *Phys. Fluids* **11**, 955–957.

LeBlond, P. H. & Mysak, L. A. 1978 *Waves in the Ocean*. Elsevier.

Le Dizès, S. 2000 Three-dimensional instability of a multipolar vortex in a rotating flow. *Phys. Fluids* **12**, 2762–2774.

McEwan, A. D. & Robinson, R. M. 1975 Parametric instability of internal gravity waves. *J. Fluid Mech.* **67**, 667–687.

Majda, A. J. & Grote, M. J. 1997 Model dynamics and vertical collapse in decaying strongly stratified flows. *Phys. Fluids* **9**, 2932–2940.

Majda, A. J. & Shefter, M. G. 1998 Elementary stratified flows with instability at large Richardson number. *J. Fluid Mech.* **376**, 319–350.

Mansour, N. N. & Lundgren, T. S. 1990 Three-dimensional instability of rotating flows with oscillating axial strain. *Phys. Fluids* A **2**, 2089–2091.

Mied, R. P. 1976 The occurrence of parametric instabilities in finite-amplitude internal gravity waves. *J. Fluid Mech.* **78**, 763–784.

Miyazaki, T. 1993 Elliptical instability in a stably stratified rotating fluid. *Phys. Fluids* A **5**, 2702–2709.

Miyazaki, T. & Fukumoto, Y. 1992 Three-dimensional instability of strained vortices in a stably stratified fluid. *Phys. Fluids* A **4**, 2515–2522.

Pierrehumbert, R. T. 1986 Universal short-wave instability of two-dimensional eddies in an inviscid fluid. *Phys. Rev. Lett.* **57**, 2157–2159.

Riley, J. J. & Lelong, M.-P. 2000 Fluid motions in the presence of strong stable stratification. *Annu. Rev. Fluid Mech.* **32**, 613–657.

Sekerzh-Zen'kovitch, S. Ya. 1983 Parametric resonance in a stratified liquid in a container undergoing vertical vibrations. *Sov. Phys. Dokl.* **28**, 445–446.

Smith, L. M. & Waleffe, F. 2002 Generation of slow large scales in forced rotating stratified turbulence. *J. Fluid Mech.* **451**, 145–168.

Staquet, C. & Sommeria, J. 2002 Internal gravity waves: from instabilities to turbulence. *Annu. Rev. Fluid Mech.* **34**, 559–593.

THORPE, S. A. 1994 Observations of parametric instability and breaking waves in an oscillating tilted tube. *J. Fluid Mech.* **261**, 33–45.

WALEFFE, F. 1990 On the three-dimensional instability of strained vortices. *Phys. Fluids* A **2**, 76–80.

YAKUBOVICH, V. A. & STARZHINSKII, V. M. 1975 *Linear Differential Equations with Periodic Coefficients,* vol. 2. Wiley.

ZHUKOVSKII, N. E. 1892 Conditions for finiteness of integrals of equations $y'' + py = 0$. *Mat. Sbornik* **16**, 582–591.